Sliding Mode Propulsion System Control for Two wheels Electric Vehicle Drive

A. Nasri[1], A. Hazzab[1], I. K. Bousserhane[1], S. Hadjeri[2]
[1] Bechar University, B.P 417 Bechar (08000), Algeria. E-mail: *nasriab1978@yahoo.fr.*
[2] University of Djillali Liabes, B.P 98 Sidi Bel-Abbes (22000), Algeria.

Abstract : In this paper novel propulsion system control stability is presented. The present work introduces multi-converter multi-machine systems (MMS), the proposed propulsing system consists of two induction motors (IM) that ensure the drive of the two back driving wheels. The proposed control structure-called independent machines- for speed control permit the achievement of an electronic differential. The electronic differential system ensures the robust control of the vehicle behaviour on the road it also allows controlling independently every driving wheel to turn at different speeds in any curve. Our electric vehicle sliding mode control's simulated in Matlab SIMULINK environment, the results obtained present the efficiency of the proposed control with no overshoot, the rising time is perfected with good disturbances rejections comparing with the classical control law**.**

***Key words* : Electric** vehicle, Electronic differential, induction machine, propulsion system, sliding mode control.

I. INTRODUCTION

Electric vehicles (EVs) are developing fast during this decade due to drastic issues on the protection of environment and the shortage of energy sources. While commercial hybrid cars have been rapidly exposed on the market, fuel-cell-powered vehicles are also announced to appear in 5–10 years. Researches on the power propulsion system of EVs have drawn significant attention in the automobile industry and among academics. EVs can be classified into various categories according to their configurations, functions or power sources. Pure EVs do not use petroleum, while hybrid cars take advantages of energy management between gas and electricity [1]**.**

Indirectly driven EVs are powered by electric motors through transmission and differential gears, while directly driven vehicles are propelled by in-wheel or, simply, wheel motors [2]. The basic vehicle configuration of this research has two directly driven wheel motors installed and operated inside the driving wheels on a pure EV. These wheel motors can be controlled independently and have so quick and accurate response to the command that the vehicle chassis control or motion control becomes more stable and robust, compared to indirectly driven EVs. Like most research on the torque distribution control of wheel motor, wheel motors [3] proposed a dynamic optimal tractive force distribution control for an EV driven by four wheel motors, thereby improving vehicle handling and stability.

The researchers assumed that wheel motors were all identical with the same torque constant; neglecting motor dynamics the output torque was simply proportional to the input current with a prescribed torque constant.

In this paper, a sliding mode decoupling controller for electric vehicle control is proposed. The reminder of this paper is organized as follows:

Section II reviews the principle components of the Electric traction chain modeling .Section III shows the indirect field-oriented control (IFOC) of induction motor. Section IV shows the development of sliding mode controllers design for Electric vehicle .The proposed structure of the studied propulsion system is given in the section V. Section VI gives some simulation results of different studied cases. Finally, the conclusion is drawn in section VII.

II. ELECTRIC TRACTION SYSTEM ELEMENTS MODELLING

Figure 1 represents the general diagram of an electric traction system using an induction motor (IM) supplied by voltage inverter [8].

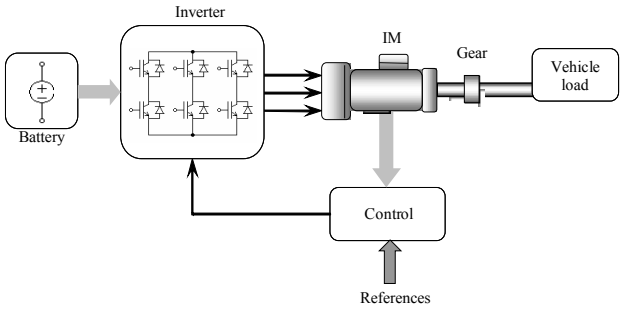

Fig.1: Electrical Propulsion system traction chain

A. Energy source

The battery considered in this paper is of the Lithium-Ion accumulator's battery for which a simple model is assumed. Therefore, a simplified version of the complex battery model reported in [9] is used

B. Static converter

In this electric traction system, we use an inverter to obtain three balanced alternating current phases with variable frequency from the current battery.

$$\begin{bmatrix} v_{an} \\ v_{bn} \\ v_{cn} \end{bmatrix} = \frac{U_{dc}}{2} \begin{bmatrix} 2 & -1 & -1 \\ -1 & 2 & -1 \\ -1 & -1 & 2 \end{bmatrix} \begin{bmatrix} S_a \\ S_b \\ S_c \end{bmatrix} \quad (1)$$

The logic S_i of the switches are obtained by comparing the control inverter signals with the modulation's signal.

C. Traction motor

The used motor is a three phase induction motor type (IM)

supplied by an inverter voltage controlled with Pulse Modulation Width (PWM) techniques. A model based on circuit equivalent equations is generally sufficient in order to make control synthesis. The dynamic model of three-phase, Y-connected induction motor can be expressed in the *d-q* synchronously rotating frame as [6, 7]:

$$\begin{cases} \frac{di_{ds}}{dt} = \frac{1}{\sigma.L_s}\left(-\left(R_s+\left(\frac{L_m}{L_r}\right)^2.R_r\right).i_{ds}+\sigma.L_s.\omega_e.i_{qs}+\frac{L_m.R_r}{L_r^2}.\phi_{dr}+\frac{L_m}{L_r}.\phi_{qr}.\omega_r+V_{ds}\right) \\ \frac{di_{qs}}{dt} = \frac{1}{\sigma.L_s}\left(-\sigma.L_s.\omega_e.i_{ds}-\left(R_s+\left(\frac{L_m}{L_r}\right)^2.R_r\right).i_{qs}-\frac{L_m}{L_r}.\phi_{dr}.\omega_r+\frac{L_m.R_r}{L_r^2}.\phi_{qr}+V_{qs}\right) \\ \frac{d\phi_{dr}}{dt} = \frac{L_m.R_r}{L_r}.i_{ds}-\frac{R_r}{L_r}.\phi_{dr}+(\omega_e-\omega_r)\phi_{dr} \\ \frac{d\phi_{qr}}{dt} = \frac{L_m.R_r}{L_r}.i_{qs}-(\omega_e-\omega_r)\phi_{dr}-\frac{R_r}{L_r}.\phi_{qr} \\ \frac{d\omega_r}{dt} = \frac{3}{2}\frac{P^2.L_m}{L_r.J}.(i_{qs}.\phi_{dr}-i_{ds}.\phi_{qr})-\frac{f_c}{J}.\omega_r-\frac{P}{J}.T_l \end{cases} \quad (2)$$

Where σ is the coefficient of dispersion and is given by (2):

$$\sigma = 1-\frac{L_m^2}{L_s L_r} \quad (3)$$

L_s , L_r , L_m	stator, rotor and mutual inductances;
R_s , R_r	stator and rotor resistances;
ω_e , ω_r	electrical and rotor angular frequency;
ω_{sl}	slip frequency $(\omega_e-\omega_r)$;
τ_r	rotor time constant (L_r/R_r);
P	pole pairs

D. Mechanical part.

The developed globally traction chain model based on the data uses from the Leroy-Somer Society, [4] is shown in figure 2:

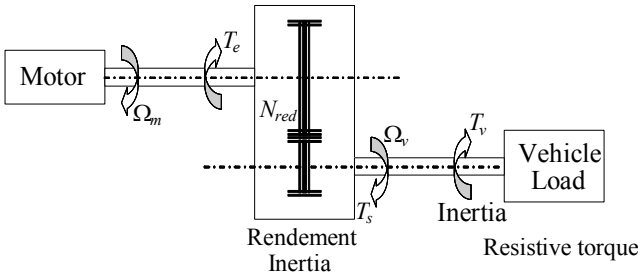

Fig.2: Electromechanical structure

1. The vehicle as load

The vehicle's considered as a load is characterized by many torques which are mostly considered as resistive torques [4, 5, 12, 13, 16, 17]. The different torques includes:

1. The vehicle inertia torque is defined by the following relationship:

$$T_{in} = J_v.\frac{dw_v}{dt} \quad (4)$$

2. The aerodynamics torque is :

$$T_{aero} = \frac{1}{2}\rho S.T_x.R_r^3.w_r^2 \quad (5)$$

3. The slope torque is given as :

$$T_{slope} = Mg.\sin\alpha \quad (6)$$

4. The maximal torque of the tire which can be opposed to the motion has the following expression:

$$T_{\max} = Mgf_r.R_r \quad (7)$$

We obtain finally the total resistive torque:

$$T_v = T_{slope}+T_{tire}+T_{aero} \quad (8)$$

2. Gear

The speed gear ensures the transmission of the motor torque to the driving wheels. The gear is modelled by the gear ratio, the transmission efficiency and its inertia.

The mechanical equation is given by:

$$J_e\frac{dw_m}{dt}+fw_m = p(T_{em}-T_r) \quad (09)$$

With:

$$T_r = \frac{1}{\eta N_{red}}T_v \quad (10)$$

$$J_e = J+\frac{J_v}{\eta N_{red}^2} \quad (11)$$

The modelling of the traction system allows the implementation of some controls such as the vector control and the speed control in order to ensure the globally system stability.

III. VECTOR CONTROL

The main objective of the vector control of induction motors is, to control independently the flux and he torque as DC machines, this is done by using a *d-q* rotating reference frame synchronously with the rotor flux space vector [6, 7, 15]. In ideally field-oriented control, the rotor flux linkage axis is forced to align with the *d*-axes, and it follows that [6, 7, 15]:

$$\phi_{rq} = \frac{d\phi_{rq}}{dt} = 0 \quad (12)$$

$$\phi_{rd} = \phi_r = cons\tan t \quad (13)$$

Applying the result of (12) and (13), namely the indirect field-oriented control, the torque equation become analogous to the DC machine and can be described as follows:

$$T_e = \frac{3}{2}\frac{p\cdot L_m}{L_r}\cdot\phi_r\cdot i_{qs} \quad (14)$$

And the slip frequency can be given as follow:

$$\omega_{sl} = \frac{1}{\tau_r}\frac{i_{qs}^*}{i_{ds}^*} \quad (15)$$

Consequently, the dynamic equations (1) yield:

$$\frac{di_{ds}}{dt} = -\left(\frac{R_s}{\sigma L_s} + \frac{1-\sigma}{\sigma \tau_r}\right) i_{ds} + \omega_e i_{qs} + \frac{L_m}{\sigma L_s L_r \tau_r}\phi_{rd} + \frac{1}{\sigma L_s} V_{ds} \quad (16)$$

$$\frac{di_{qs}}{dt} = -\left(\frac{R_s}{\sigma L_s} + \frac{1-\sigma}{\sigma \tau_r}\right) i_{qs} - \omega_e i_{ds} + \frac{L_m}{\sigma L_s L_r \tau_r}\phi_{rd} + \frac{1}{\sigma L_s} V_{ds} \quad (17)$$

$$\frac{d\phi_r}{dt} = \frac{L_m}{\tau_r} i_{ds} - \frac{1}{\tau_r}\phi_{rd} \quad (18)$$

$$\frac{d\omega_r}{dt} = \frac{3}{2}\frac{P^2 L_m}{J L_r} i_{qs}\phi_{rd} - \frac{f_c}{J}\omega_r - \frac{P}{J}T_l \quad (19)$$

The decoupling control method with compensation is to obtain the inverter output voltages such that [10]:

$$V_{ds}^* = \left(K_p + K_i \frac{1}{s}\right)\left(i_{ds}^* - i_{ds}\right) - \omega_e \sigma L_s i_{qs}^* \quad (20)$$

$$V_{qs}^* = \left(K_p + K_i \frac{1}{s}\right)\left(i_{qs}^* - i_{qs}\right) + \omega_e \sigma L_s i_{ds}^* + \omega_r \frac{L_m}{L_r}\phi_{rd} \quad (21)$$

According to the above analysis, the indirect field-oriented control (IFOC) [6, 7, 15] of induction motor with current-regulated with PWM inverter control system can reasonably presented by the block diagram shown in the Fig. 3.

In this step we use the classical regulator for IFOC tuning control parameter.

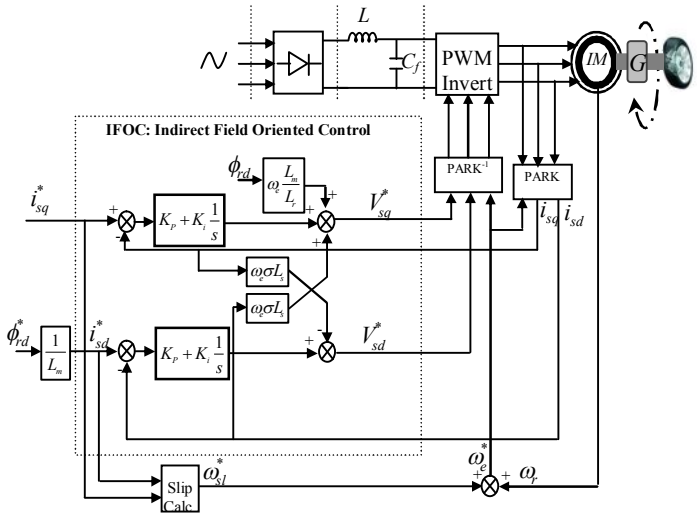

Fig. 3: IFOC strategy for an EV induction motor.

IV. SLIDING MODE CONTROL

Sliding modes is phenomenon may appear in a dynamic system governed by ordinary differential equations with discontinuous right-hand sides. It may happen that the control as a function of the system state switches at high frequency, this motion is called sliding mode. It may be enforced in the simplest tracking relay system with the state variable *x(t)* [7 ,8 , 9, 10, 11]:

$$\frac{\partial x}{\partial t} = f(x) + u \quad (22)$$

With the bounded function $f(x)$

$|f(x)| < f_0$; f_0 is constant and the control as a relay function of the tracking error $e = r(t) - \frac{\partial x}{\partial t}$; $r(t)$ is the reference input and u is given by:

$$u = \begin{cases} +u_0 & ;if \quad e > 0 \\ -u_0 & ;if \quad e < 0 \end{cases} \quad (23)$$

Or: $u = u_0 sign(e)$; u is constant.

Figure.4 shows the relay control scheme:

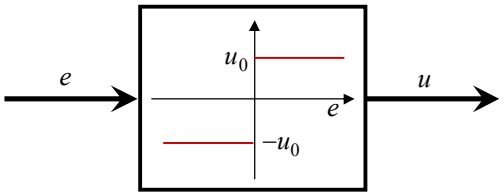

Fig.4: relay control

The values of e and $\frac{\partial e}{\partial t} = \dot{e} = \dot{r} - f(x) - u_0 sign(e)$

According to Lyapunov stability criteria the system's stable if it does verify the following condition: $e.\dot{e} < 0$

By means that we have the different signs if $u_0 > f_0 + \left|\dot{r}\right|$.

And finally u_0 must be positive constant.

IV.1. *Design of sliding mode speed and current controller*

The speed error is de fined by [8, 9, 10, 11]:

$$e = w_{ref} - w \quad (24)$$

The derivative of the sliding surface can be given as:

$$\dot{s}(\omega) = \dot{\omega}_r^* - \dot{\omega}_r \quad (25)$$

From the equation (24) and (2), we can obtain:

$$\dot{s}(\omega_m) = \dot{\omega}_m{}^* - \left(\frac{3}{2}\frac{P^2 L_m \phi_{dr}^*}{J L_r} i_{qs} - \frac{f_c}{J}\dot{\omega}_m - \frac{P}{J}T_l\right) \quad (26)$$

The current control is given by:

$$i_{qs} = i_{qs}^{equ} + i_{qs}^n \quad (27)$$

To avoid the chattering phenomenon produced by the *Signs* function we use the Saturation function *Sat* in the discontinuous control defined as follow:

$$sat\left(\frac{S}{\phi}\right) = \begin{cases} \frac{S}{\phi} & ; \quad if \quad \left|\frac{S}{\phi}\right| < 1 \\ Sign\left(\frac{S}{\phi}\right) & ; \quad if \quad \left|\frac{S}{\phi}\right| > 1 \end{cases}$$

Where ϕ is the boundary layer thickness.

The discontinuous control action can be given as:

$$i_{qs}^n = k_{iqs} \cdot sat\left(s(\omega)/\phi_\omega\right) \quad (28)$$

k_{iqs}: Positive constant.

The current control is defined by:

$$i_{qs}^{equ} = \frac{2}{3}\frac{JL_r}{P^2 L_m \phi_{dr}^*}\left(\dot{\omega}_m^* + \frac{f_c}{J}\omega_m + \frac{P}{J}T_l\right) \quad (29)$$

The figure.5 shows the SMC control strategy scheme for the electric traction chain.

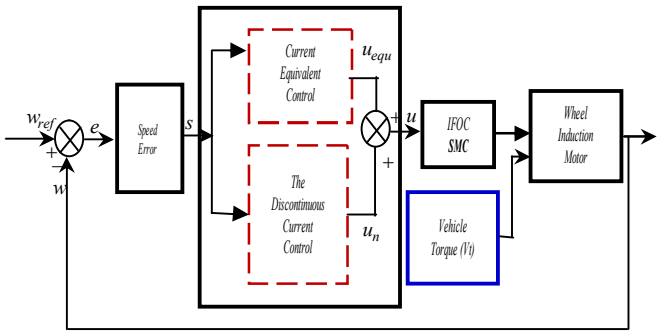

Fig.5: the SMC control strategy scheme

For the IFOC tuning parameters we need two surfaces S_1 and S_2 the first for the i_{ds} regulator and the second for i_{qs} regulator respectively where:

$$s_1 = i_{ds}^* - i_{ds} \tag{30}$$

$$s_2 = i_{qs}^* - i_{qs} \tag{31}$$

The derivate of S_1 can be given as:

$$\dot{s}_1 = \dot{i}_{ds}^* - \dot{i}_{ds}$$

from equation (2) and (30) we can obtain :

$$\dot{s}_1 = \dot{i}_{ds}^* - \left[-\left(\frac{R_s}{\sigma L_s} + \frac{1-\sigma}{\sigma \tau_r} \right) i_{ds} + \omega_e i_{qs} + \frac{L_m}{\sigma L_s L_r \tau_r} \phi_{rd} + \frac{1}{\sigma L_s} V_{ds} \right]$$

The virtual voltage controller V_{ds} is given by:

$$V_{ds} = V_{ds}^{equ} + V_{ds}^{n} \tag{32}$$

The voltage discontinuous control V_{ds}^n is defined as:

$$V_{ds}^n = k_1 \cdot sat\left(s_1 / \phi_1\right) \tag{33}$$

According to Lyapunov stability criteria [10] our speed loop system's sable if: $s_1 \dot{s}_1 < 0$ by means that K_1 is positive constant.

The equivalent control V_{ds}^{equ} is given as:

$$V_{ds}^{equ} = \sigma . L_s \left(\dot{i}_{ds}^* + \frac{1}{\sigma . L_s} \left(R_S + R_r \left(\frac{L_m}{L_r} \right)^2 \right) . i_{ds} - w_s . i_{qs} - \frac{L_m . R_r}{\sigma . L_s L_r^2} \phi_r^* \right) \tag{32}$$

The derivate of S_2 can be given as:

$$\dot{s}_2 = \dot{i}_{qs}^* - \dot{i}_{qs}$$

From equation (2) and (31) we can obtain:

$$\dot{s}_2 = \dot{i}_{qs}^* - \left[-\left(\frac{R_s}{\sigma L_s} + \frac{1-\sigma}{\sigma \tau_r} \right) i_{qs} - \omega_e i_{ds} + \frac{L_m}{\sigma L_s L_r \tau_r} \phi_{rd} + \frac{1}{\sigma L_s} V_{qs} \right]$$

The voltage controller V_{qs} is given by:

$$V_{qs} = V_{qs}^{equ} + V_{qs}^{n} \tag{33}$$

The V_{qs}^{equ} equivalent control actions defined as:

$$V_{qs}^{equ} = \sigma . L_s . [i^*_{qs} + \omega_s . i_{ds} + \frac{1}{\sigma . L_s} \left(R_s + R_r \left(\frac{L_m}{L_r} \right)^2 \right) . i_{qs} + \frac{L_m}{\sigma L_s L_r} \phi_r^* \omega_m] \tag{34}$$

The voltage discontinuous control V_{ds}^n is defined as:

$$V_{qs}^n = k_2 \cdot sat\left(s_2 / \phi_2\right) \tag{35}$$

For the same reason condition of K_1 :

K_2 is positives constant.

V. STRUCTURE OF THE STUDIED SYSTEM

The general scheme of the driving wheels control is represented by figure 7. It's an electric vehicle, which the back vehicle wheels are controlled independently by two IM.

The reference blocks must provide the speed references of each motor taking into consideration informations from the different sensors.

V.1. Speed references computation.

It is possible to determine the speed references versus the requirements of the driver. When the vehicle arrives at the beginning of a curve, the driver applies a curve angle on each driving wheels [13,16,17]. The electronic differential acts immediately on the two motors reducing the driving wheel speed situated inside the curve, and increases the speed of the driving wheel situated outside the curve. The driving wheels angular speeds are:

$$w_{rR} = \frac{V_h}{R_r} + k_b . \Delta w \tag{36}$$

$$w_{rL} = \frac{V_h}{R_r} - k_b . \Delta w \tag{37}$$

with k_b = +1 corresponding to a choice of the direction of the wheel, (-1) for the right turn , and (+1) for the left turn. The driving wheels speed variation is imposed by the trajectory desired by the driver and it's given by:

$$\Delta w = \frac{d_w}{2} \frac{\sin(\delta + \beta)}{l_w . \cos \delta} . \frac{V_h}{R_r} \tag{38}$$

The relation between α which is the curve angle given by the driver wheel and δ of the real curve angle of the wheels is given by: $\delta = \frac{\alpha}{k_d}$ (39)

The figure 6 shows the vehicle geometry of the studied system.

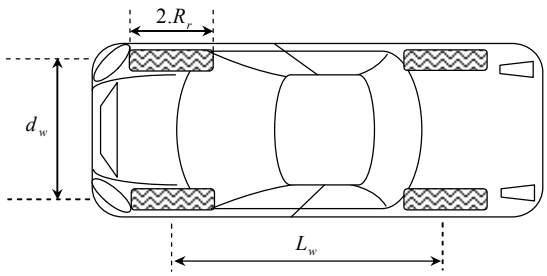

Fig.6 : vehicle geometry

where k_d is the gear ratio. A proportionality coefficient between δ and β which is the vehicle slip angle is defined

by : $\beta = k.\delta$ (40)

The speeds references of the two motors are:

$w^*_{mR} = N_{red}.w_{rR}$ (41)

$w^*_{mL} = N_{red}.w_{rL}$ (42)

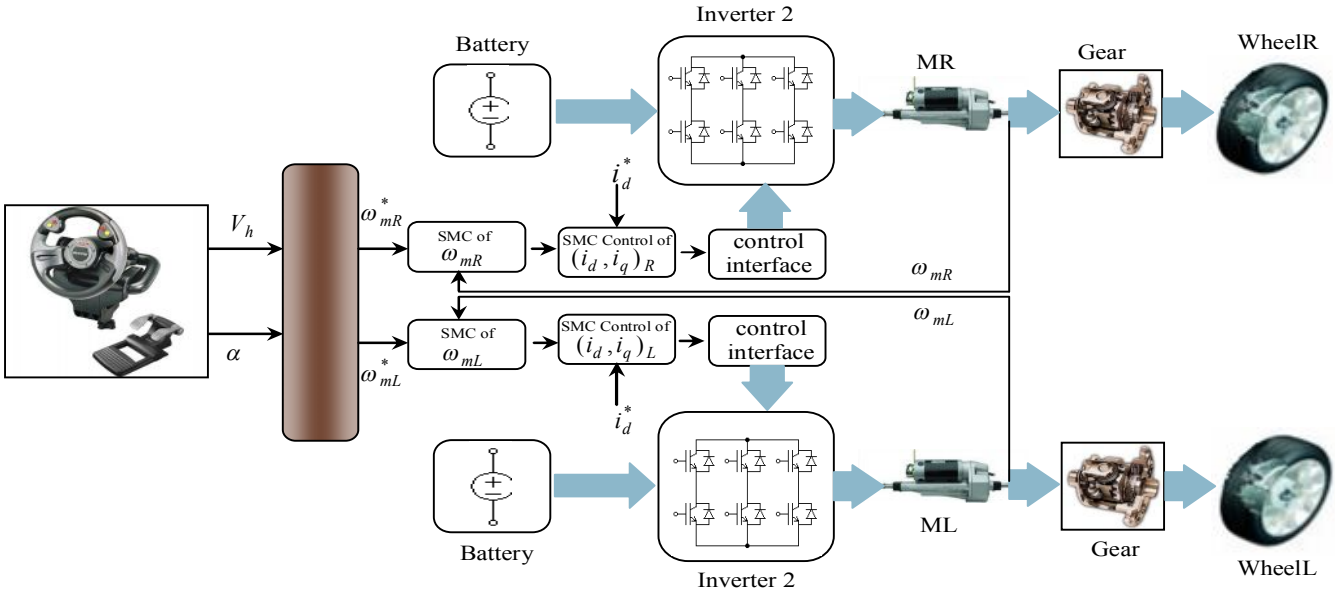

Fig.7 : The driving wheels control of the studied propulsion system.

VI. SIMULATION RESULTS

In order to characterise the driving wheel system behaviour, simulations were carried using the model of figure.7. They show vehicle speed variation for PI and the Sliding mode controllers.

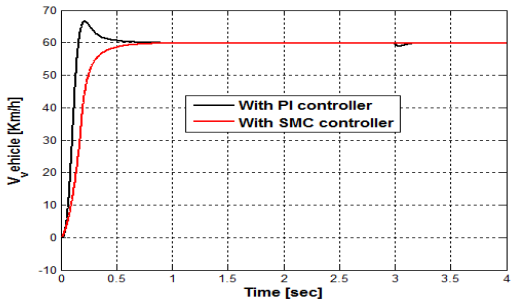

Fig. 8: vehicle speed for two controller cases

In order to simplify the control algorithm and improve the control loop robustness, instead of using classical control, we use the sliding mode control [9, 10, 11, 18]. The advantage of this control is its robustness, its capacity to maintain ideal trajectories for two wheels control independently and ensure good disturbances rejections with no overshoot and stability of vehicle perfected ensured with the speed variation and less error speed.

To compare the effect of disturbances in the speed loop for law control in two cases, figure.8 shows the system response.

We can summaries the results of the two control laws in the table given bellow:

Table 1: Performances of the PI & SMC controllers in the speed loop response

Results	*Rising time [Sec]*	*Overtaking [%]*	*Steady state error [%]*	*Disturbance application time (slope torque)*
PI	0.8895	11.6666	0	At 3 Sec
SMC	0.7932	0	0	At 3 Sec

From the figure.8 and the table we can say that: the effect of the disturbance is neglected in the case of the sliding mode control. It appears clearly that the classical control with PI controller is easy to apply. However the control with sliding mode controllers offers better performances in both of the overshoot control and the tracking error.

In addition to these dynamic performances, it respects the imposed constraints by the driving system such as the robustness of parameter variations

A. Case of straight way

- Flat road with 10% slope at 60km/h speed

In this test, the system is submitted to the same speed

step. The driving wheels speeds stay always the same and the road slope does not affect the control of the wheel and the sliding mode control act immediately on the speed loop's and rejects the disturbance and give's more and more efficiency to the electronic differential output references. Only a change of the developed motor torque is noticed. We can say the slope effect results in a high improvement in the electromagnetic motor torque left and right of each motor and it's sensitize the motorization to develop efforts in order to satisfy the electric traction chain demand . The system behaviour of theses speeds is illustrated by figures 9.1, 9.2, figures 9.5. and 9.4 describe he electromagnetic left and right variations. The resistant torques are shown in figures 9.3.

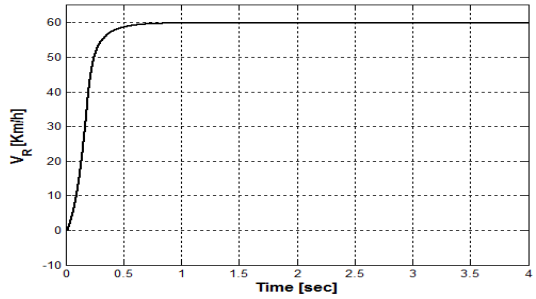

Fig. 9.1: Right Wheel speed

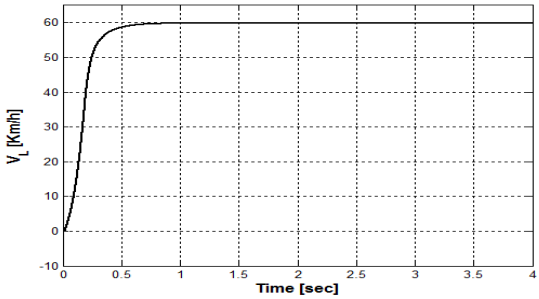

Fig. 9.2: left Wheel speed

We can summaries the results o the straight way driven wheels in the following tables:

Table 2: Performances of the PI & SMC controllers in vehicle speed loop

Results	Δw	V^*_{refL}	V^*_{refR}	α	Vh	V_{wL}	V_{wR}
PI	0	60	60	0	60	60.87	60.87
SMC	0	60	60	0	60	60	60

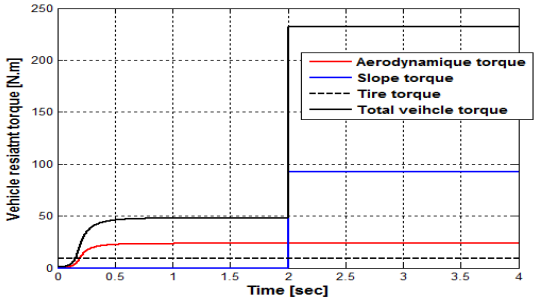

Fig. 9.3: Resistive Torques

All vehicle torques variation results are illustrated in this table:

Table 3: Performances of the SMC controller

Results	***Total vehicle torques (T_v)***	***Tire torque (Ttire)***	***Aerodynamique torque (Taero)***	***Slope torque (Tslope)***
Maximum value [Nm]	124.10	9.10	25	90
Time application [Sec]	Permanent	Permanent	Permanent	2

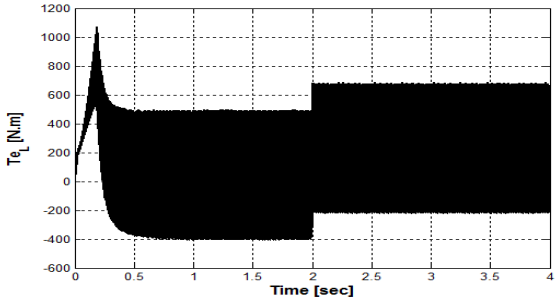

Fig. 9.4: left motor Electromagnetic Torque

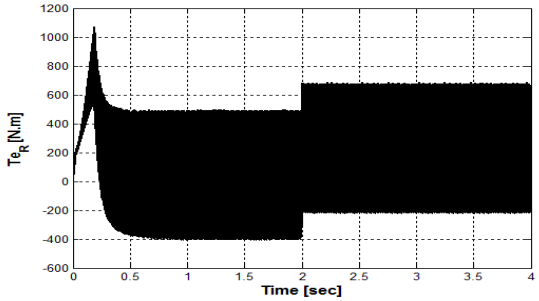

Fig. 9.5: right motor Electromagnetic Torque

B. Case of curved way

-Curved road at right side with speed of 60km/h

The vehicle is driving on a curved road on the right side with 60*km*/*h* speed. The assumption is that the two motors are not disturbed. In this case the driving wheels follow different paths, and they turn in the same direction but with different speeds.

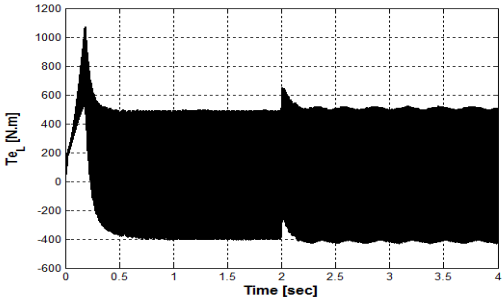

Fig. 10.1: left motor Electromagnetic Torque

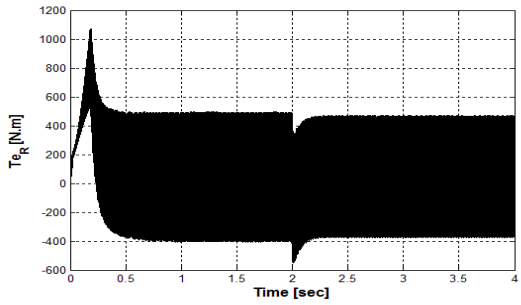

Fig. 10.2: right motor Electromagnetic Torque

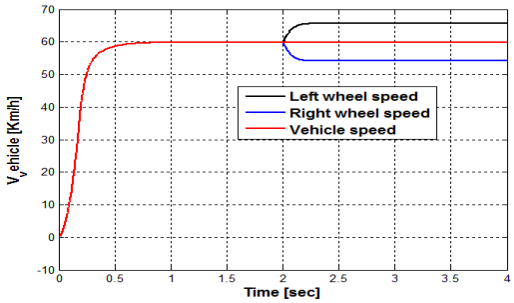

Fig. 10.3: vehicle speed in right turn in curved way

Also we can summaries our curved way response results On the following table

Table 4: Performances of the SMC controller in the vehicle speed loop

Results	**PI**	**SMC**
Δv [Km/h]	5	5
V^*_{refL} [Km/h]	65.74	65
V^*_{refR} [Km/h]	54.26	55
Time curve [Sec]	2	2
Curve angle α [°]	5.81	5.81
Vh [Km/h]	60	60
V_{wL} [Km/h]	65.6	65
V_{wR} [Km/h]	54.15	55

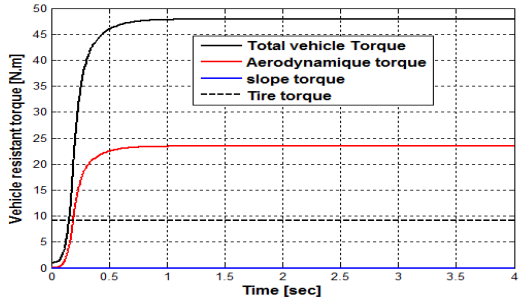

Fig. 10.4: Resistive Torques in right turn in curved way

We can summaries all electric vehicle torques in the following table:

Table 5: Performances of the SMC controller on the vehicle torques response

Results	***Total vehicle torques (T_v)***	***Tire torque (Ttire)***	***Aerodynamique torque (Taero)***	***Slope torque (Tslope)***
Maximum value [Nm]	33.8	9.8	24	0
Time application [Sec]	Permanent	Permanent	Permanent	No Application

The electronic differential acts on the two motor speeds by decreasing the speed of the driving wheel on the right side situated inside the curve, and on the other hand by increasing the wheel motor speed in the external side of the curve. The sliding mode control ensure the stability of the propulsing system by maintaining the motorization error speed equal zeros and gives a good rising time and no over tracking error too. The behaviour of these speeds is given by figure 10.3, figure 10.4 shows the electric vehicle resistant torques and figures 10.1and 10.2 shows the electromagnetic torques.

VII. Conclusion

The research outlined in this paper has demonstrate the feasibility of an improved vehicle stability which uses two independent back drive wheels for motion by using the sliding mode control

The proposed 'independant machine' control approach structure applied to a propulsing system by the sliding mode speed control ensure the disturbance rejection. The results obtained by simulation show that this structure permits the realization of an robust control loop speed based on Lyapunov switching surface with a good dynamic and static performances of electric traction chain. The proposed sliding mode model controls the driving wheels speeds with high accuracy either in flat roads or curved ones in each case. The disturbances do not affect the performances of the driving motor wheels stability.

Appendix

Table 6: Electric vehicle Parameters

Te	Motor traction torque	247 Nm
J_e	Moment on inertia of the drive train	7.07Kgm^2
R_w	Wheel radius	0.36m
a	Total gear ratio	10.0
η	Total transmission efficiency	0.93
M	Vehicle mass	3904Kg
f_e	Bearing friction coefficient	0.001
K_d	Aerodynamic coefficient	0.46
A	Vehicle frontal area	3.48 m^2
f_v	Vehicle friction coefficient	0.01
α	Grade angle of the road	rad
L_w	Distance between two wheels and axes	2.5m
d_w	Distance between the back and the front wheel	1.5m

Table 7: Induction Motors Parameters

R_r	Rotor winding resistance (per phase)	0.003 Ω
Rs	Stator winding resistance (per phase)	0.0044 Ω
L_s	Stator leakage inductance (per pohase)	16.1 µH
L_m	Magnetizing inductance (per phase)	482 µH
L_r	Rotor leakage inductance (per phase)	12.9 µH
f_c	Friction coefficient	0.0014
P	Number of poles	4
N	Based speed	2885 rpm
	Rated power	100 hp

Table8: Symbols, Designation and Units.

Symbols	**Nomenclature**	**units**
R_r	Rotor resistance	Ω
R_s	Stator resistance	Ω
P	Pole pairs	
L_s	Stator inductance	µH
L_r	Rotor inductance	µH
L_m	Mutual inductance	µH
J	Rotor inertia	$Kg.m^2$
J_e	Moment of inertia of the drive train	$Kg.m^2$
J_v	Vehicle inertia	$Kg.m^2$
T_{em}	Electromagnetic torque	Nm
T_v	Vehicle torque	Nm
T_{slope}	Slope torque	Nm
T_{aero}	Aerodynamique torque	Nm
T_{tire}	Tire torque	Nm
T_{in}	Inertia vehicle torque	Nm
N_{red}	Report of speed gear	%
G	Gear box	
η	Transmission efficiency	%
L_w	Distance between two wheels	m
d_w	Distance between the back and the front wheel	m
ρ	Air density	Nm^{-2}
S	Frontal vehicle surface	m^2
C_x	Aerodynamic drag coefficient	
M	Vehicle mass	Kg
g	Gravitational acceleration	N/m
α	Angle grade of road	rad
f_r	Wheels Rolling resistance coefficient	
U_{dc}	Battery voltage	Volt
K_b	Choice of direction coefficient	Rad/sec
ΔW	Angular speed variation given by electronic differential	Rad/sec
W_{rR}	Right wheel angular speed	Rad/sec
W_{rL}	Left wheel angular speed	Rad/sec
W^*_{mR}	Right wheel angular speed of reference	Rad/sec
W^*_{mL}	Left wheel angular speed of reference	rad
δ	Reel angle wheel curve's	rad
β	Vehicle slip angle	rad
K_{iqs}	Stator current coefficient of speed law control	
φ	Boundary layer	
K_1	Stator voltage control coefficient parameter	
K_2	Stator direct voltage control coefficient parameter	
Sat	Saturation surface	
IFOC	Indirect field oriented control	
SMC	Sliding mode control	

REFERENCES

[1]. A.Poursamad, M. Monazeri."Design of Genetic-Fuzzy Control Strategy for Parallel Hybrid Electric Vehicles ", Control Engineering Practice,doi:10.1016/j.conengprac.2007.10.003.

[2]. Y. Pien Yang, C.Pin Lo "Current Distribution Control of Dual Directly Driven Wheel Motor for Electric Vehicles", Control Engineering Practice, Vol n°16, 2008. pp.1285-1292.

[3]. He. Hori, Y.Kamachi, M.Walters."Future Motion Control to be realized by in-Wheel Motored Electric Vehicle" .The 31 St Annual Conference of The IEE Industrial Electronics Society .IECON 2005.Raliegh South Carolina, USA.

[4]. B.C.Besselink. »Computer Controlled Steering System for Vehicles having Two Independently Driven Wheels», Computers and Electronics in Agriculture, Vol39, 2003, pp.209-226.

[5]. Multon, B., Hirsinger, L.: Problème de la motorisation d'un véhicule Electrique (Motorization problem of an electric vehicle), EEA " Voiture et Electricité" ("Car and Electricity") 24 et 25 Mars 1994, Cachan (France).

[6]. J. Jung, K. Nam, "A Dynamic Decoupling Control Scheme for High-Speed Operation of Induction Motors", IEEE Trans. on Ind. Elect. Vol. 46/01 (1999).

[7]. M. Zhiwen, T. Zheng, F. Lin and X. You, "a New Sliding-Mode Current Controller for Field Oriented Controlled Induction Motor Drives", IEEE Int. Conf. IAS (2005), pp. 1341-1346, 2005.

[8]. Yoichi, H., Yasushi, T., and Yoshimasa, T.: Traction control of electric vehicle: Basic experimental results using the test EV "UOT Electric march". IEEE. Transactions on Industry Applications. Vol.34, No.5. September/October 1998. p. 1131-1138.

[9]. S. Sadeghi, J. Milimonfared, M. Mirsalim, M. Jalalifar, "Dynamic Modeling and Simulation of a Switched Reluctance Motor in Electric Vehicle", in Proc,2006 ICIEA Conf.

[10]. A. Mezouar,M.K Fellah,S.Hadjeri. "Adapive Sliding Mode Observer for Induction Motor Using Two-Time Scale Aproach, Electric Power Research 16.2008.1323-1336.

[11]. A.Tahour,Hamza.Abid.A.Aissaoui,"Speed Control of Switched Reluctance Motor Using uzzy Sliding Mode",Advances in Electrical an Compuer Engineering ,Vol,8.15,Number 1(29),2008.

[12]. C. E.Barbier, B. Negarede and H. L.meyer "Global Control Strategy Optimization Of An Asynchronous Drive System For An Electric Vehicle", Control Eng.Practice, vol.4.n°.8, pp.1053-1066, 1996.

[13]. James Larminie, "Electric Vehicle Technology Explained", Editted by John Wiley and John Lowry, England, 2003.

[14]. R. -J. Wai, "Adaptive Sliding-Mode Control for Induction Servomotor Drives", IEE Proc. Elecrr. Power Appl., 2000,147, pp. 553-562.

[15]. C. M. Lin and C. -F. Hsu, "Adaptive Fuzzy Sliding-Mode Control for Induction Servomotor Systems", IEEE Transactions on Energy Conversion, vol. 19, n°2, June 2004, pp. 362-368

[16]. M. Ehsani, K.M. Rahman, H.A. Toliyat: Propulsion System Design of Electric and Hybrid Vehicle, IEEE Tran. On industrial Electronics, Vol. 44, No.1, February 1997.

[17]. H. Huang," Electrical two speed transmission and advanced control of electric vehicles", Phd thesis, New Brunswick university, June 1998.

[18]. A.Boushema. C. Chaigne,N.Bensiali,"Design of Speed Adapation Law in Sensorless Control of Induction Motor in Regenerating Mode, ", Science Direct, Vol. 15.2007.pp.847-863.